KeAi

CHINESE ROOTS
GLOBAL IMPACT

Contents lists available at ScienceDirect

#### Petroleum Science

journal homepage: www.keaipublishing.com/en/journals/petroleum-science



#### Original Paper

## Research on the pollution and damage mechanism of drilling fluid on casing during ultra-deep well drilling process



Han-Xuan Song <sup>a, b</sup>, Shi-Ling Zhang <sup>c</sup>, Xiang-Wei Chen <sup>a, b</sup>, Kiyingi Wyclif <sup>a, b</sup>, Ji-Xiang Guo <sup>a, b, \*</sup>, Rui-Ying Xiong <sup>a, b</sup>, Li Wang <sup>a, b</sup>

- <sup>a</sup> Unconventional Petroleum Research Institute, China University of Petroleum, Beijing, 102249, China
- <sup>b</sup> State Key Laboratory of Petroleum Resource and Prospecting, China University of Petroleum (Beijing), Beijing, 102249, China
- <sup>c</sup> CNPC Engineering Technology R&D Company Limited, Beijing, 102200, China

#### ARTICLE INFO

# Article history: Received 31 July 2024 Received in revised form 19 December 2024 Accepted 19 December 2024 Available online 21 December 2024

Edited by Jia-Jia Fei

Keywords: Ultra-deep well Casing contamination Corrosion Tribology Drilling fluid

#### ABSTRACT

In drilling ultra-deep wells, the drilling fluid circulation usually causes erosion damage to downhole casing and drilling tools. However, the extent and process of this damage to the downhole tools is intricate and less understood. In order to systematically evaluate and clarify this damage process for different types of drilling fluid contamination, this research uses a high-temperature drilling fluid damage device to simulate the damage caused to the casing/drilling tools by various drilling fluid under a field thermal gradient. The results show that the drilling fluid residues are mainly solid-phase particles and organic components. The degree of casing/tool damage decreases with an increase in bottom hole temperature, and the casing/tool is least damaged within a temperature range of 150-180 °C. Moreover, the surface of the casing/tool damaged by different types of drilling fluid shows different roughness, and the wettability of drilling fluid on the casing/tool surface increases with an increase in the degree of roughness. Oil-based drilling fluid have the strongest adhesion contamination on casing/drilling tools. In contrast, polysulfonated potassium drilling fluid and super-micro drilling fluid have the most potent erosion damage on casing/drilling tools. By analyzing the damage mechanism, it was established that the damage was mainly dominated by the abrasive wearing from solid-phase particles in concert with corrosion ions in drilling fluid, with solids producing many abrasion marks and corrosive ions causing a large number of pits. Clarifying drilling fluid's contamination and damage mechanism is significant in guiding the wellbore cleaning process and cutting associated costs.

© 2024 The Authors. Publishing services by Elsevier B.V. on behalf of KeAi Communications Co. Ltd. This is an open access article under the CC BY license (http://creativecommons.org/licenses/by/4.0/).

#### 1. Introduction

Ultra-deep well drilling technology is widely used in western China (Ma et al., 2022; Pu et al., 2022), and wellbore contamination caused by drilling fluid during the drilling process has been increasingly emphasized (Liu et al., 2022; Palimi et al., 2022). Currently, the drilling fluid used for ultra-deep well drilling are mainly water-based and oil-based (Jiang et al., 2022; Sun et al., 2022). During the circulation of drilling fluid, due to the complex downhole environment (Deng et al., 2022; Guo et al., 2021), the drilling fluid residual stuck on the casing wall causes wear or corrosion to the casing as well as the drilling tools (Gautam et al., 2022) which leads to complex downhole accidents (Ji et al., 2022)

\* Corresponding author. E-mail address: guojx003@126.com (J.-X. Guo). 2023). The contamination was first reported in the Gulf of Mexico and the Norwegian continental shelf (Berg et al., 2006; Brege et al., 2012; Quintero et al., 2011). The adhesion of drilling fluid affects the progress of downhole operations, and the photographs taken at the site are shown in Fig. 1.

The research on the damage mechanism for drilling fluid on the casing is superficially understood (Etrati et al., 2020; Yanagisawa et al., 2021). Therefore, exploring the damage mechanism of drilling fluid on the casing can provide theoretical guidance for protecting the casing/drilling tool and cleaning the casing walls and drilling tools (Wang et al., 2016; Zhang et al., 2022). Currently, scholars mainly focus on the wear or corrosion of drilling fluid on metal surfaces during the contact process between drilling fluid and downhole casing/tools using the disc friction method at room (Davoodi et al., 2023). Mao et al. (2020) investigated the friction damage behavior between oil-based drilling fluid and casing using the disc friction method. The study analyzed the effects of different



Fig. 1. Downhole drilling fluid contamination in the field.

oil/water ratios for oil-based drilling fluid on the variability of casing abrasion. When the proportion of oil phase increases, the wear of drilling fluid on the casing decreases. Zhang et al. (2018) quantified the residual mud on the casing using the fluorescent dye method and determined the correlation between the roughness of the metal surface and the residual drilling fluid. The results showed a good correlation between the thickness of the residual drilling fluid and the surface roughness. Palimi et al. (2022) investigated the effect of glycerol-based additives in drilling fluid on frictional corrosion of carbon steel surfaces. Analysis of the lubrication film on the carbon steel surface showed that the additive can significantly increase drilling fluid performance, and the carbon steel surface corrosion and wear were significantly reduced. Luo et al. (2023) investigated the tribological properties of oilbased drilling fluid in different temperature environments and explored the fluidity and interfacial wear using reactive molecular dynamics. The results showed that the friction fluctuation degree is higher at high temperatures than at low temperatures, increasing the wear region at the contact friction interface. Humood et al. (2019) studied the friction and wear characteristics of oil-based drilling fluid on casing drilling tools in long horizontal sections and concluded that drilling fluid additives have a specific mitigating effect on friction and wear.

Generally, to an extent, current studies have explored the damage caused by drilling fluid. However, due to the complexity of the downhole environment (Guo et al., 2019; Jia et al., 2020), the existing studies do not systematically and comprehensively evaluate this damage process and mechanism. With the aim to shorten this research gap, this research examines the casing/drilling tool damage due to various types of drilling fluid at different temperatures in ultra-deep wells. The study also derives a damage mechanism for drilling fluid on downhole casing/drilling tools to guide the oil field's downhole cleaning operations.

#### 2. Experiment and methods

#### 2.1. Experimental samples and materials

#### 2.1.1. Different drilling fluid types

High-density water-based and oil-based drilling fluid used in ultra-deep wells were selected for this research study (Luo et al., 2023; Mikhienkova et al., 2022), and the different types of drilling fluid are shown in Fig. 2. Water-based drilling fluid are categorized into polysulfonated potassium (Poly-potassium) drilling fluid (Barite Powder Aggravator) and super-micro drilling fluid (Iron Powder Aggravator).

The performance of drilling fluid slurries is shown in Table 1.

#### 2.1.2. Metal samples for wellbore and tools

P110 steel was used for the wellbore, and 42CrMo was used for the drilling tools (Fig. 3). The element composition for P110 and 42CrMo steel specimens are given in Table 2, respectively.

#### 2.2. Fouling characteristics of the drilling fluid

The particle size analysis for the different drilling fluid was carried out using a particle size analyzer (OMCC-Topsizer). The microflow morphology of drilling fluid was observed using the OLYMPUS Zeiss Primo Star Biomicroscope (Carl Zeiss, Germany). An electron microscope SEM (Quanta 200 F) was used to observe the surface of P110 steel and 42CrMo alloy contaminated by drilling fluid. The micro adhesion behavior between the solid phase of the drilling fluid and the steel sheet was analyzed.

The solids content in the drilling fluid was calculated using the mass difference method. The drilling fluid sample of mass as  $m_1$ , was dried in a vacuum oven (DZF-6020) at 105 °C for 2 h to remove the water, and the mass after drying was recorded as  $m_2$ . The dried

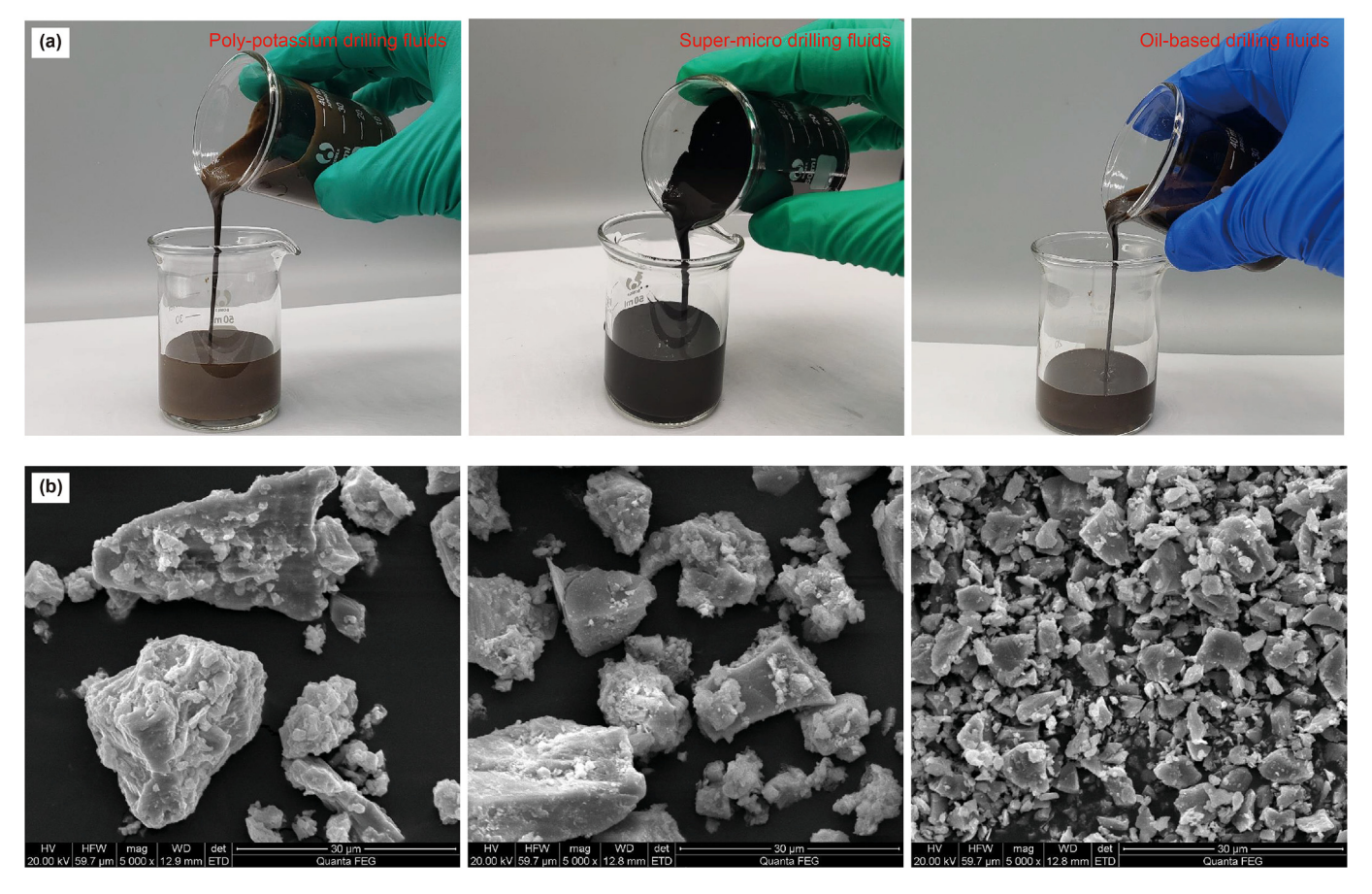


Fig. 2. (a) Flow state observations of different types of drilling fluids; (b) Microanalysis of drilling fluid solid phase particles.

**Table 1**Performance parameters of drilling fluid.

Drilling fluid types	$\rho$ , g/cm <sup>3</sup>	AV, mPa∙s	<i>PV</i> , mPa·s	<i>YP</i> , mPa·s	G'/G"	ES, V
Poly-potassium	1.9	28	10	18	6/14	/
Super-micro	2.1	35	21	14	7/15	/
Oil-based	1.8	30	26	4	8/15	800



Fig. 3. P110 and 42CrMo steel test specimens.

sample was taken out and calcinated to remove the organic matter, and the mass of the sample after calcination was recorded as  $m_3$ . The drilling fluid water content  $W_1$  and the organic content ratio  $W_2$  were calculated using Eqs. (1) and (2), respectively.

$$W_1 = \frac{m_1 - m_2}{m_1} \tag{1}$$

$$W_2 = \frac{m_2 - m_3}{m_1} \tag{2}$$

#### 2.3. High-temperature corrosion and wear damage

#### 2.3.1. Relative flow velocity calculation

The corrosion and wear due to drilling fluid on the casing mainly occur during annular volume circulation between the wellbore and tools.

The relative flow rate of drilling fluid on the casing surface is mainly determined through the drilling fluid displacement (*V*, L/s). A schematic diagram of drilling fluid backflow is shown in Fig. 4. Drilling data from a selected ultra-deep well in Tarim Oilfield was used for the calculation. The well parameters are provided in Table 3.

The inner diameter of the wellbore  $r_3$  was calculated using Eq. (3).

$$r_3 = r_2 - l_3 \times 2 \tag{3}$$

Equation (4) was used to calculate the wellbore annular area, s.

**Table 2**The chemical composition of P110 steel (balance is Fe) and 42CrMo steel (balance is Fe).

	Elemental	С	Si	Mn	Cr	Mo	P	S	Cu	Ni	V
P110 steel	Mass fraction, %	<0.29	<0.27	<0.50	<0.90	<0.18	<0.02	<0.01	<0.20	<0.20	<0.08
42CrMo steel	Mass fraction, %	<0.45	<0.37	<0.80	<1.2	<0.25	< 0.035	< 0.035	1	1	<0.08

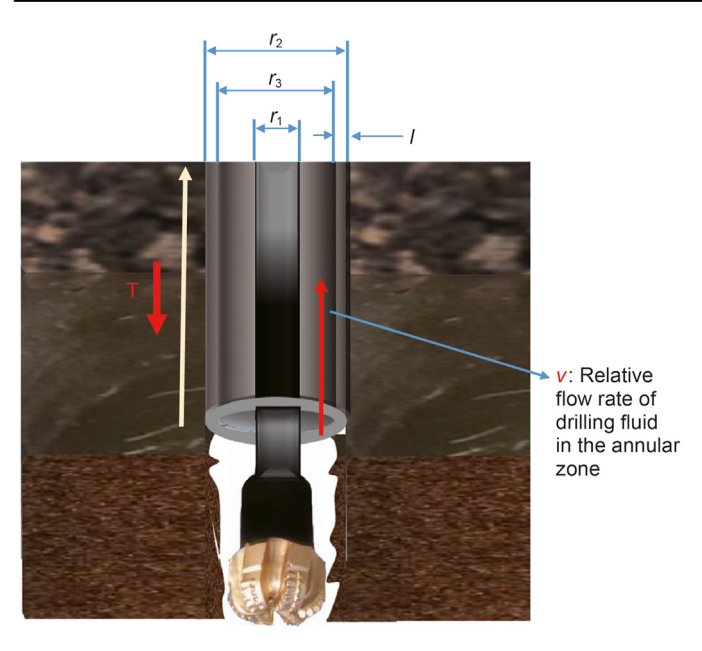


Fig. 4. Simulation of drilling fluid circulation.

$$s = \pi r_3^2 - \pi r_1^2 \tag{4}$$

The flow rate of drilling fluid in the wellbore annulus was calculated using Eq. (5).

$$\nu = \frac{V}{S} \tag{5}$$

#### 2.3.2. High-temperature corrosion and wear test

Throughout the entire drilling cycle in ultra-deep wells, different depths have different temperatures, which have a certain degree of impact on the contact between drilling fluid and casing.

Regarding the corrosion and wear issues of drilling fluid on casing and drilling tools, an in-house high-temperature corrosion and wear tester developed by China University of Petroleum (Beijing) was used for testing at four temperatures: 90, 150, 180, and 200  $^{\circ}$ C. By rotating the steel plate and generating relative motion with the drilling fluid, the required temperature for the reaction is provided through a sealed heating chamber, and the required pressure is provided through N<sub>2</sub>, the simulation of the real situation of downhole drilling fluid is achieved. The high-temperature corrosion and wear experimental device is shown in Fig. 5.

#### 2.4. Principles and calculations of damage on metal surfaces

## 2.4.1. Calculation of the degree of damage to metal surfaces In an attempt to evaluate the degree of metal surface damage

**Table 3** Drilling data.

Well return depth, mCasing nameCasing O.D., mmDrill pipe diameter, mmCirculation rate, L/s3070Technical casing193.68101.617

caused by drilling fluid, the weight change method was used to quantitatively assess the synergistic effect of wear and corrosion. The wear and corrosion rates (W) of P110 and 42CrMo steel specimens were obtained at different temperatures (i.e., at different pipe sections). The calculation formula is given in Eq. (6).

$$W = \frac{m_0 - m_1}{m_0} \tag{6}$$

where W is the damage rate,  $m_0$  and  $m_1$  are the original and post-reaction masses.

A laser confocal profilometer (Marsurf cm-select) was used to construct a three-dimensional metal surface under the synergistic effect of damage, and the degree of damage was observed.

#### 2.4.2. Electrochemical tests

The electrochemical workstation (CHI660E) was used to conduct corrosion evaluation experiments on metal steel plates for casing. The electrolytic cell used for the tests was a flat plate corrosion electrolytic cell. The electrodes used in the experiment are as follows: the working electrode is a P110-type, 42CrMo-type specimen with a contact area of 1 cm<sup>2</sup> with the corrosion medium; the Ag/AgCl electrode was the reference electrode.

#### 2.4.3. Determination of the coefficient of friction

A hydraulic friction wear testing machine (MRS-100) was used to test the coefficient of friction of the system under different drilling fluid media, and analyze the degree of friction on the casing by different types of drilling fluid.

#### 2.4.4. Calculation of roughness of metal surfaces after reaction

Data points were extracted after 3D modeling of the steel specimens, and the roughness of the specimen surfaces was calculated. Then, the roughness of the steel alloy specimens was compared under different damage conditions.

The principle of roughness calculation is shown in Fig. 6, the arithmetic mean deviation of the contours ( $R_a$ ) (arithmetic mean of the absolute deviation of the contours within the sampling length) in the calculation formula was used to represent the roughness of the metal sample surface (Feng et al., 2020).

#### 2.4.5. Wettability transition dynamics of alloys' surface

A contact angle measuring instrument (JY-82C-N2) was used to test the wettability of the alloys' surface before and after wear and corrosion to get the corresponding contact angle of the alloy plates.

#### 2.5. Observation of corrosion/wear changes on metal surfaces

An energy spectrum analyzer was used to analyze the composition of the reacted metal surface material to obtain the corresponding reactants. Scanning field emission scanning electron microscopy (SU8010) was used to microscan the surface of the reaction surface and observe the corrosion pits and wear marks.

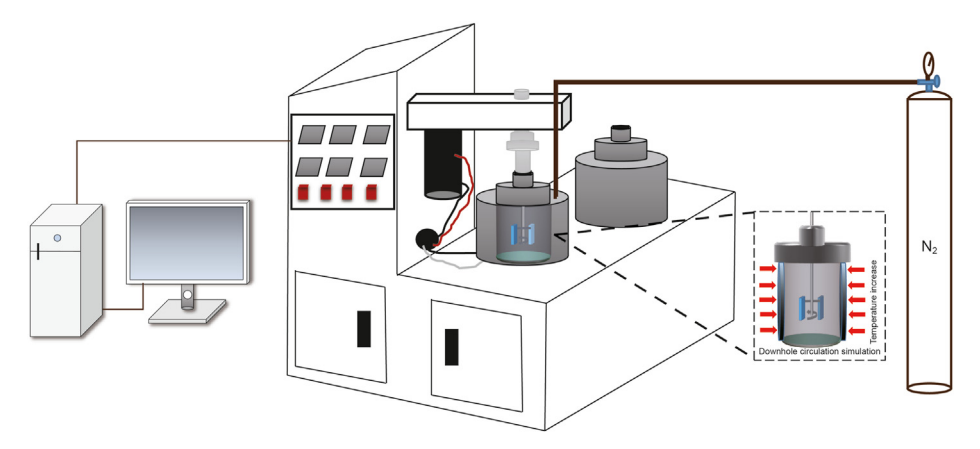


Fig. 5. High-temperature corrosion and wear test machine.

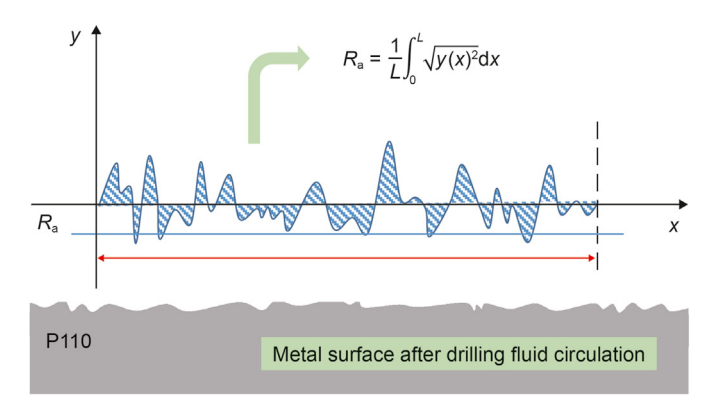


Fig. 6. Principle of calculation of contour arithmetic mean deviation  $R_{\rm a}$ .

The corrosion products on the metal surface were examined through microscopic analysis. The friction force of particles on the casing in the pipeline was studied using mechanical analysis to reveal the causes of casing damage due to drilling fluid.

#### 3. Results and discussion

#### 3.1. Characterization of casing fouling by drilling fluid

The fouling properties for each fluid were determined through analysis of the different types of drilling fluid on casing surfaces. The results are shown in Figs. 7–9, respectively.

As can be seen from Fig. 7, the oil-based drilling fluid has a high content of solid phase, with 60.5% by mass, while 31.5% is organic phase. Through microscopic observation of its fouling state, it was found that the surface of the solid phase is covered with an oil film and that the residual oil-based drilling fluid is more tightly adhered to the casing and tools.

Using the polysulfonated potassium drilling fluid, it was observed that the solid phase content of this drilling fluid is 71.4%, and the proportion of organic component content is 2.2% (Fig. 8). Under microscopic observation, it is found that the clay mineral content in potassium-based polysulfonate drilling fluid is relatively high, mainly due to the mixed deposition of clay minerals with barite powder, but it does not closely adhere to the metal surface of the casing and tool.

In super-micro drilling fluid, the solid content is about 84.2% and the organic content is 1.9% (Fig. 9). Under microscopic observation, it is found that many fine particles in the super-micro drilling fluid

adhere closely to the casing/drilling tool. The main component of the solid phase is micro iron powder, and the particle size analysis results show that its particle size is between 200 and 300 nm.

Different types of drilling fluid have different compositions, and their surface adhesion status and the particle size of the solid phase also vary. For casings and drilling tools, the interaction between different components and the metal surface varies, and the physicochemical reactions involved are complex and variable.

#### 3.2. Analysis of the extent of damage to metal surfaces

Using Eqs. (3)–(5), the relative rotational velocity (v) was calculated to be 1.297 m/s, and the rotational diameter of the steel sheet in the experimental apparatus was 27 mm, at a set speed of 364 r/min. The corresponding experimental parameters were computed based on the calculation results, and the related tests were conducted in the high-temperature corrosion and abrasion apparatus to calculate the corresponding damage rate (Fig. 10).

From Fig. 10(a), it can be seen that oil-based drilling fluid has less damage to the casing and drilling tool steel sheets. As the temperature increases, the change in quality decreases, indicating a reduction in the degree of damage. This is related to the oil film formed by oil-based drilling fluid on the surface of the steel sheet, which not only reduces the friction between particles and the steel sheet but also increases the corrosion resistance of the steel sheet surface. It has been confirmed that oil-based drilling fluid can effectively protect casing and drilling tools, extending their service life.

From Fig. 10(b), it can be seen that polysulfonated potassium drilling fluid causes significant damage to the casing and drilling tool steel sheet. As the temperature increases, the damage shows a decreasing trend. This is because the toughness of the metal is enhanced at high temperatures, which, to some extent, reduces wear. However, the high-temperature state intensifies the corrosion process, and the drilling fluid dumps many corrosion products on the metal surface (Jing et al., 2018), increasing the steel sheet quality(Anwar et al., 2019).

From Fig. 10(c), it can be seen that the super-micro drilling fluid causes significant damage to the casing and drilling tool steel sheets. This is because the super-micro drilling fluid contains a large amount of fine particles, resulting in severe abrasive wear. However, with the increase in temperature, the degree of wear decreases and shows a sharp downward trend at 180 °C, confirming that the toughness of the casing/drilling tool increases at high temperatures (Lin et al., 2016).

In general, different drilling fluid have varying degrees of

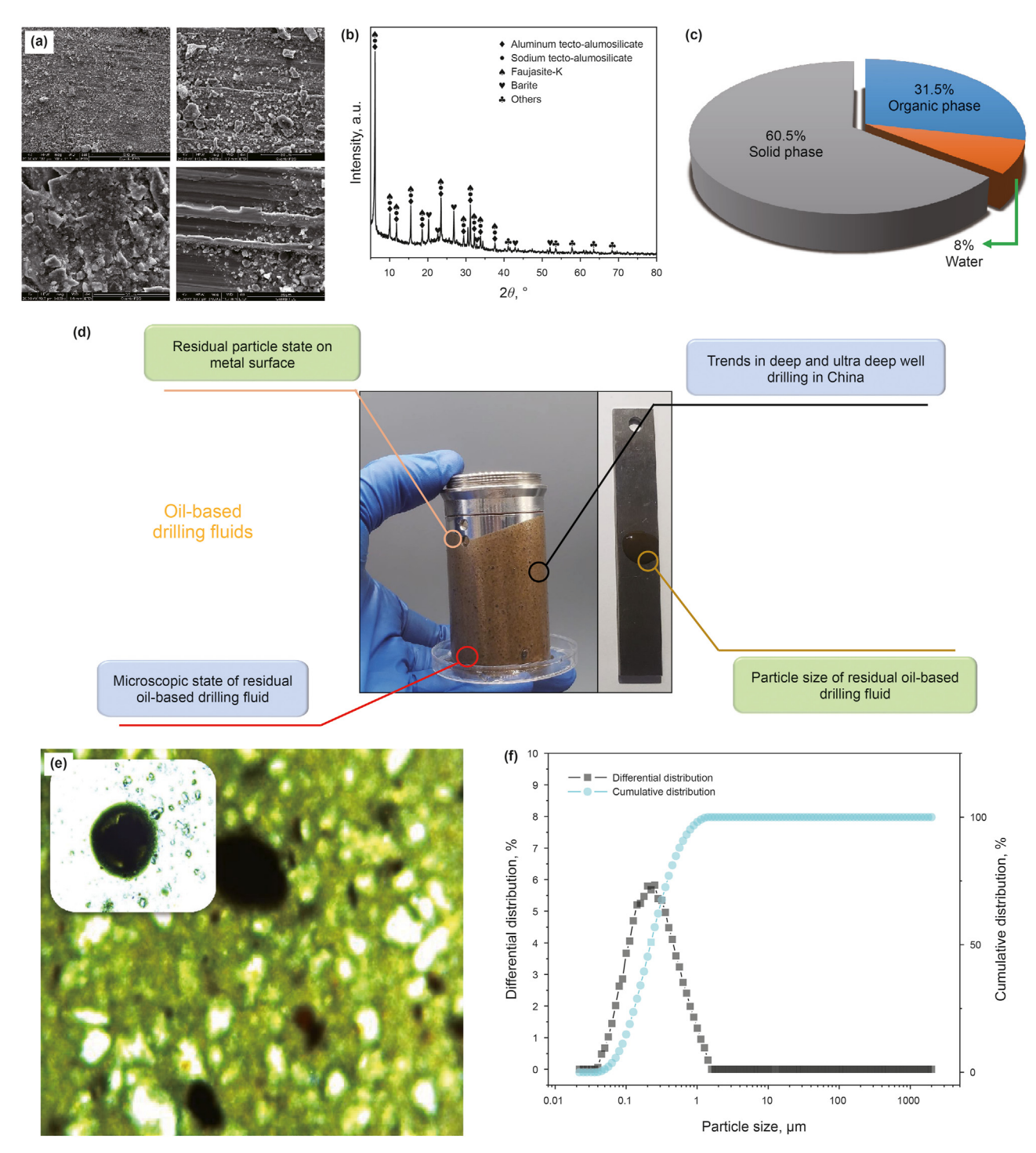


Fig. 7. (a) SEM testing of metal surfaces; (b) XRD analysis of residual oil-based drilling fluid; (c) Analysis of residual oil-based drilling fluid components; (d) Residual testing of oil-based drilling fluid; (e) Microscopic observation of oil-based drilling fluid; (f) Particle size analysis of oil-based drilling fluid.

damage to metals. The 42CrMo alloy used in the tool has stronger resistance to drilling fluid damage than the P110 alloy, and as the temperature increases, the damage from drilling fluid onto the tool and casing decreases.

3.3. Characterization of metal surface damage behavior at different well depth positions

Different temperatures are set corresponding to different well

depths to simulate downhole drilling fluid circulation, and observe the surface damage of casings and drilling tools after drilling.

Fig. 11 shows the morphology of the casing/drilling tool sample after being damaged by oil-based drilling fluid. Due to the low salt ion content and low gas solubility in the oil-based drilling fluid, the degree of metal corrosion is very minimal, and the oil phase in the oil-based drilling fluid has some lubricating effect, resulting in less abrasive wear caused by particles in the oil-based drilling fluid. The protection of the oxide film on the metal surface is relatively intact

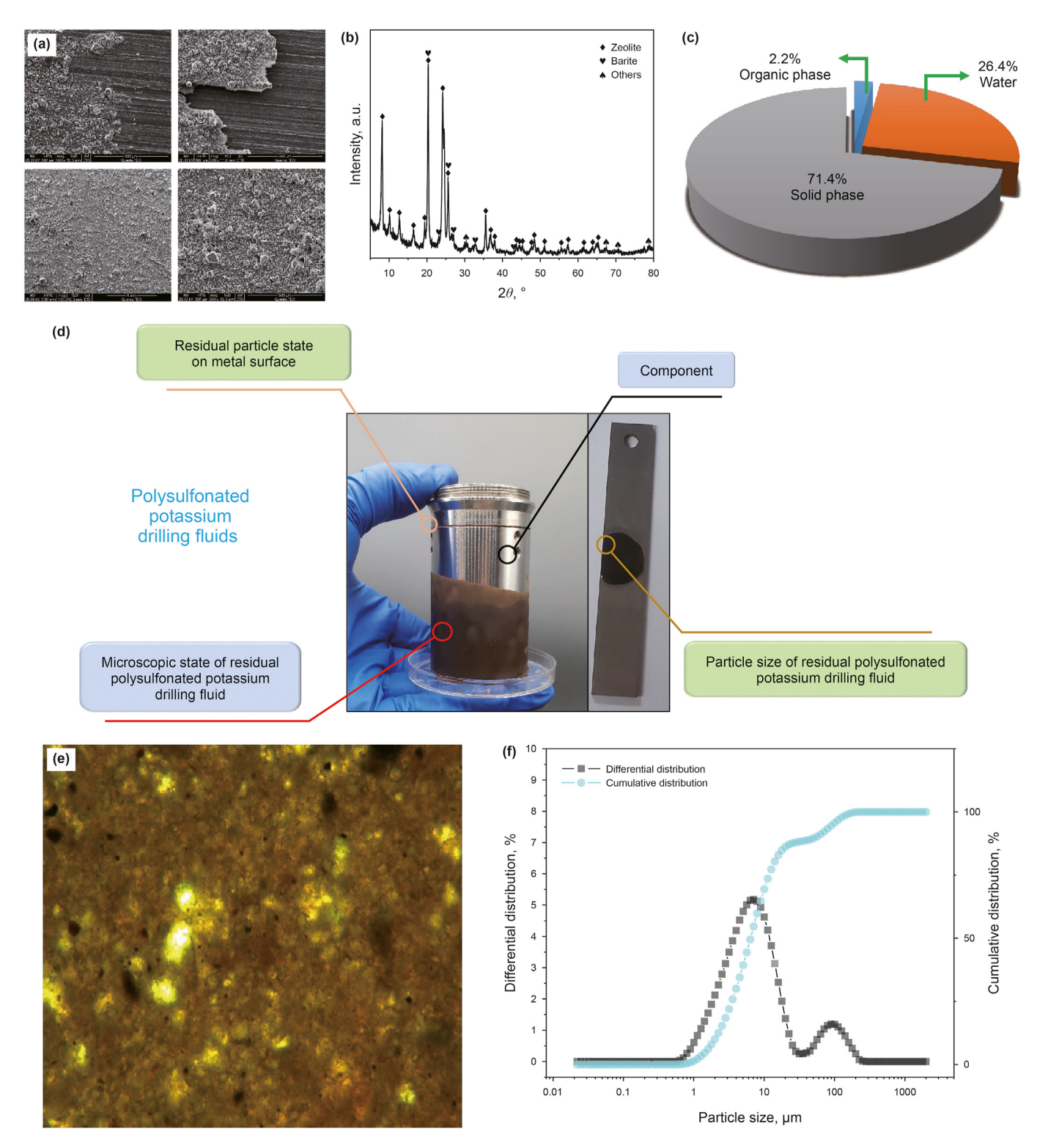


Fig. 8. (a) SEM testing of metal surfaces; (b) XRD analysis of residual polysulfonated potassium drilling fluid; (c) Analysis of residual polysulfonated potassium drilling fluid; (d) Residual testing of polysulfonated potassium drilling fluid; (e) Microscopic observation of polysulfonated potassium drilling fluid; (f) Particle size analysis of polysulfonated potassium drilling fluid.

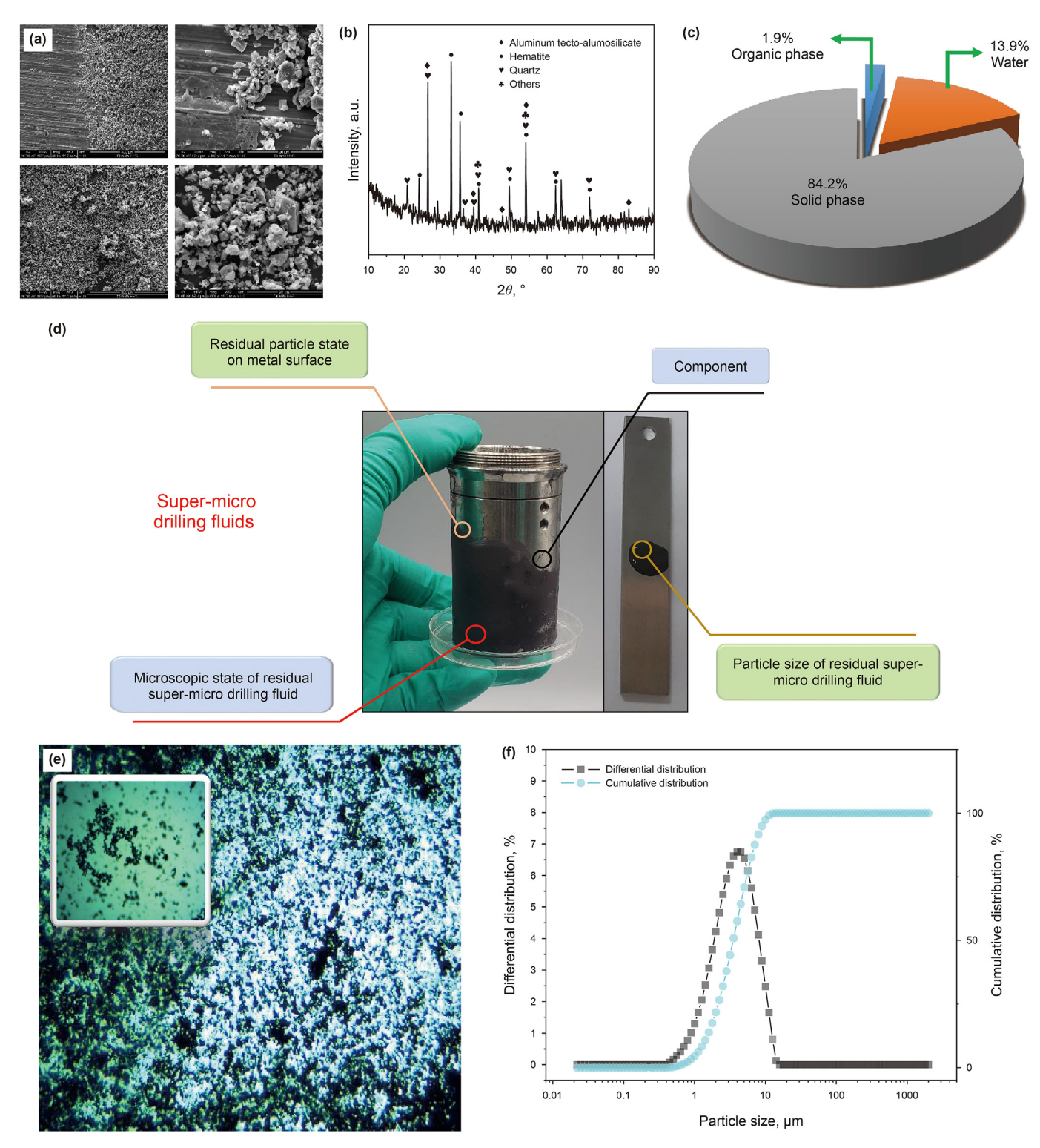
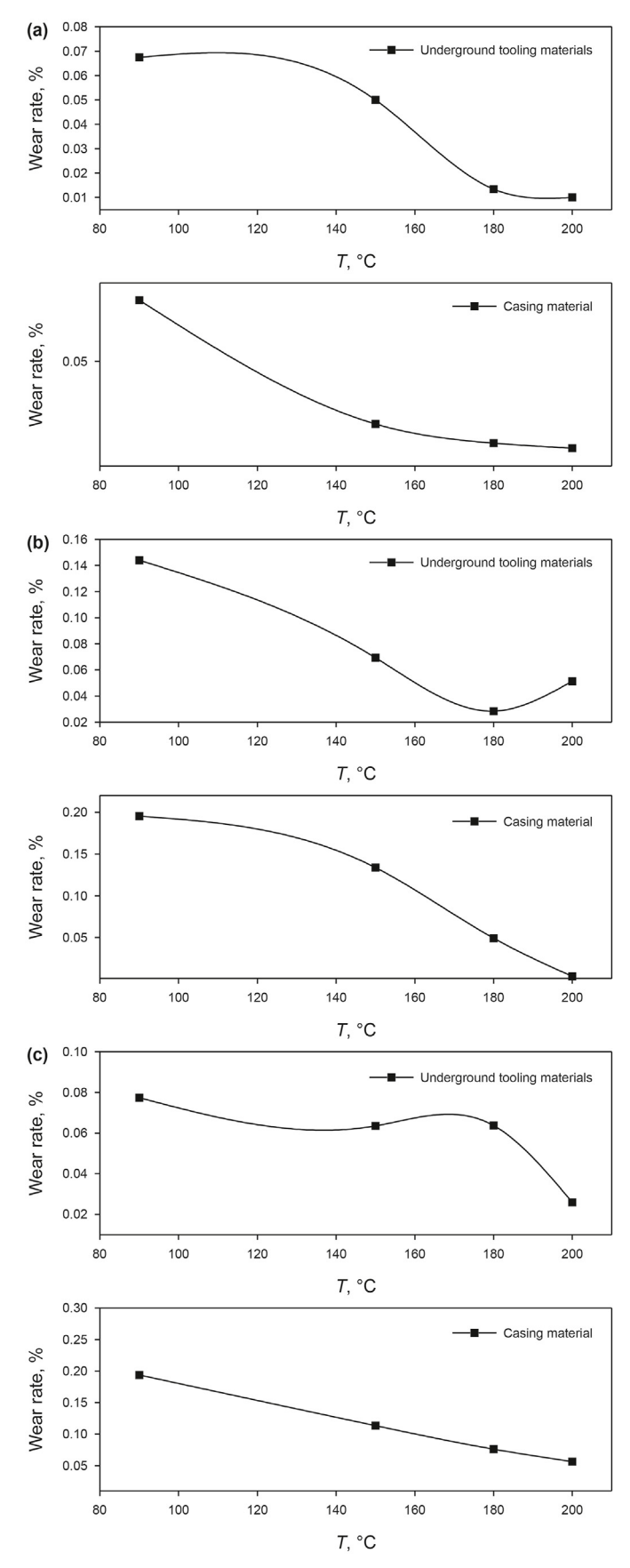


Fig. 9. (a) SEM testing of metal surfaces; (b) XRD analysis of residual super-micro drilling fluid; (c) Analysis of residual super-micro drilling fluid components; (d) Residual testing of super-micro drilling fluid; (e) Microscopic observation of super-micro drilling fluid; (f) Particle size analysis of super-micro drilling fluid.



**Fig. 10.** (a) The effect of oil-based drilling fluid damage on the quality change of steel sheets at different temperatures; (b) The effect of polysulfonated potassium drilling

during the drilling cycle. Thus, oil-based drilling fluid will create a surface oil film on the surface of the casing/drilling tool as it circulates, reducing damage to the metal surface.

Fig. 12 shows the morphology of casing/drilling tool samples damaged from polysulfonated potassium drilling fluid. Polysulfonated potassium drilling fluid contains a large amount of KCl salt, which is used to suppress the expansion of clay minerals in the clay layer. However, as an active anion, chloride ions have a preferential adsorption ability on metals, so they will preferentially adsorb on metal surfaces compared to oxygen elements. Due to their free state in the solution, they have a high probability of contact with metal surfaces, damaging the oxide film on the metal surface and exacerbating the surface damage situation.

The morphology of the casing/drilling tool sample after damage due to the super-micro drilling fluid is presented in Fig. 13. The super-micro drilling fluid contains a large amount of fine iron powder particles. During the circulation of the drilling fluid, as the temperature of the drilling fluid continues to rise and the solubility of oxygen in water decreases with the increase in the temperature, the oxide film on the metal surface decreases, and the structure is destroyed. The oxide film shows wear and detachment during the relative movement of the fine abrasive particles in the super-micro drilling fluid. This leads to severe surface wear marks, increasing the roughness of the casing/drilling tool surface and providing a good reaction site for ion corrosion.

#### 3.4. Analysis of corrosion and wear results on metal surface

Using an electrochemical workstation to test the corrosion performance of different types of drilling fluid on metal samples for casing/drilling tools, the polarization (Tafel) curve is shown in Fig. 14.

It can be seen that the curve measured by oil-based drilling fluid is much smaller than that of polysulfonated potassium drilling fluid and super-micro drilling fluid, indicating that the corrosion performance of oil-based drilling fluid is weak. Among them, polysulfonated potassium drilling fluid has the highest cathodic slope and anodic slope of the corrosion reaction, and has a strong corrosion current density, the corrosion is most obvious.

Polysulfonated potassium drilling fluid and super-micro drilling fluid use inorganic salts to inhibit the swelling of clay minerals, mainly KCl and NH<sub>4</sub>Cl, etc. The introduced ions accelerate the corrosion of the metal surface, so these two drilling fluid have a higher corrosion efficiency. Oil-based drilling fluid mainly contain a large amount of organic phase, have a low ion content, generate a small current density, and therefore have a lower corrosion rate.

Due to the differences in the composition of drilling fluid, the mutual friction effect produced by the drilling fluid on the surface of the casing/drilling tool during the circulation process also varies. The friction coefficients obtained from tests of different drilling fluid with the casing/drilling tool surfaces are shown in Fig. 15.

By comparing the friction coefficients of different drilling fluids, it was found that oil-based drilling fluids have the lowest friction coefficient, which is due to the significant lubrication provided by the oil phase components between particles and metal surfaces. This leads to less abrasive wear on the metal surface. In contrast, potassium-based poly-sulfonate drilling fluid and super-micro drilling fluid have higher friction coefficients. This means that under the same pressure, potassium-based poly-sulfonate and super-micro drilling fluid cause more severe abrasive wear on the casing.

fluid damage on the quality change of steel sheets at different temperatures; (c) The effect of super-micro drilling fluid damage on the quality change of steel sheets at different temperatures.

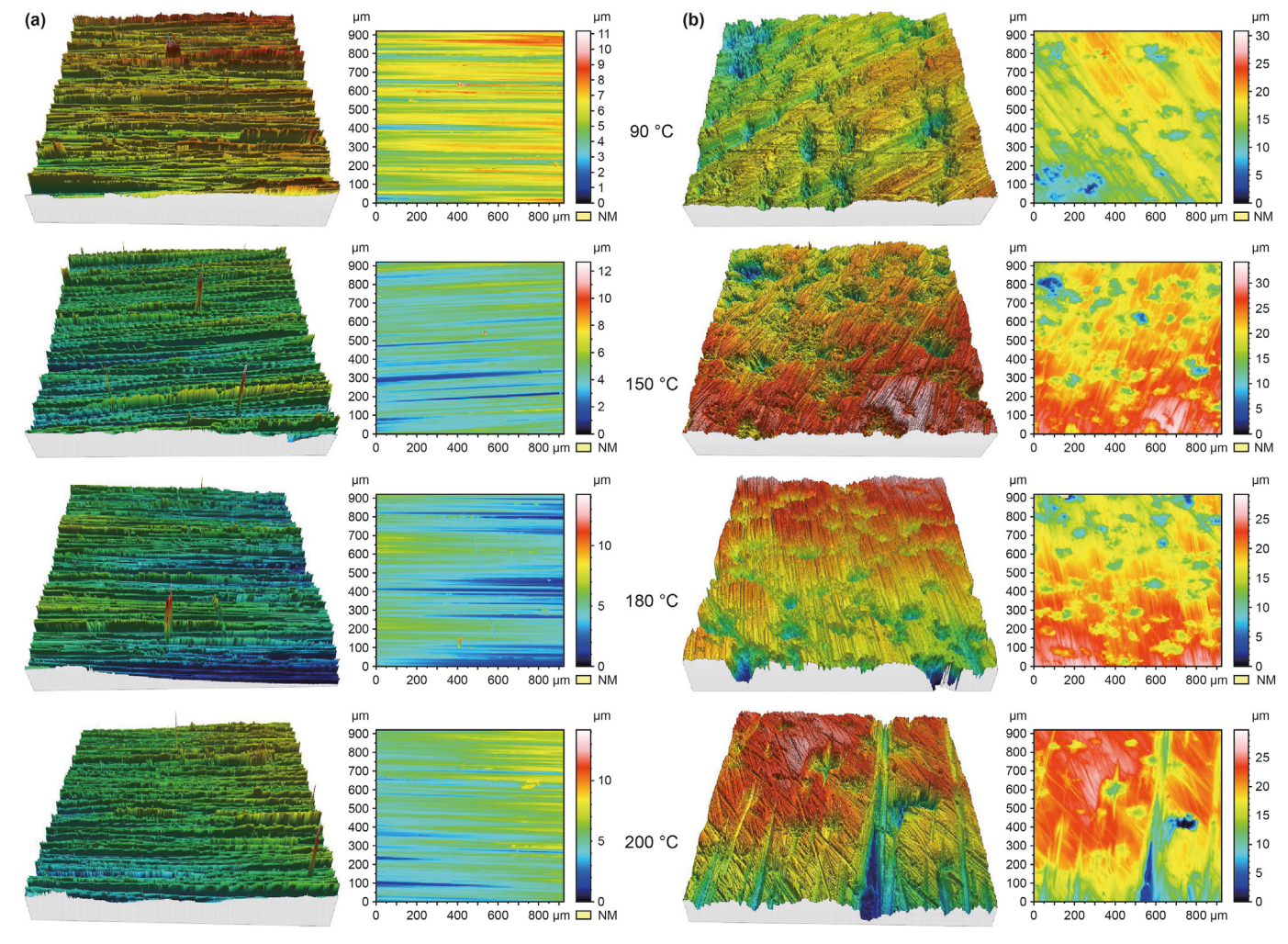


Fig. 11. (a) Casing sample morphology after oil-based drilling fluid damage; (b) Drilling tool sample morphology after oil-based drilling fluid damage.

Among them, super-micro drilling fluid have an even higher friction coefficient, which is due to the presence of a large number of micron-level particles in the fluid. Under the same pressure conditions, the smaller the particles, the greater the pressure they exert on the metal surface, leading to more severe damage. In the selection process of drilling fluid, casings, and tools, it is necessary to consider both corrosion and abrasive wear in order to maximize the lifespan of the casings and tools.

#### 3.5. Analysis of changes in metal surface roughness

The roughness data obtained through scanning calculation for the different damaged samples are shown in Figs. 16-18.

It is noticed that the surface roughness of the sample after being damaged by oil-based drilling fluid is relatively small and smooth (Fig. 16), confirming that the oil-based drilling fluid has less damage to the sample and the surface is subject to minimal corrosion and wear.

After the samples were subjected to damage from polysulfone potassium drilling fluid, the surface fluctuated drastically, which implies that the surface roughness is relatively high. The difference in surface roughness amplitudes between the P110 sample and 42CrMo sample after damage is insignificant, but the surface roughness is lower at 180 °C.

From Fig. 18, it can be seen that after damage by super-micro drilling fluid, there is a significant fluctuation on the surface of the P110 sample, but the roughness of the 42CrMo sample is less affected. This observation signifies that during the super-micro drilling fluid drilling process, the 42CrMo steel is less damaged by the drilling fluid. At 180 °C, the surface roughness of the sample is the lowest, and the surface is least affected by corrosion wear.

### 3.6. Analysis of changes in wettability of drilling fluid on metal surfaces

When the metal surface is damaged to a certain extent, the wettability of the drilling fluid on the metal surface will change to varying degrees (Wan et al., 2023). Results from the wettability test conducted on metal samples after damage from the drilling fluid are shown in Figs. 19—21.

The surface of the damaged alloy pieces subjected to oil-based drilling fluid changes slightly at different temperatures (Fig. 19). The contact angle between the oil-based drilling fluid and the damaged sample shows a weak downward trend, indicating that the adsorption between the drilling fluid and the damaged alloy piece increases, thus rendering it hard to clean.

At different temperatures, the casing/drilling tool samples exhibit different contact angles with polysulfonated potassium

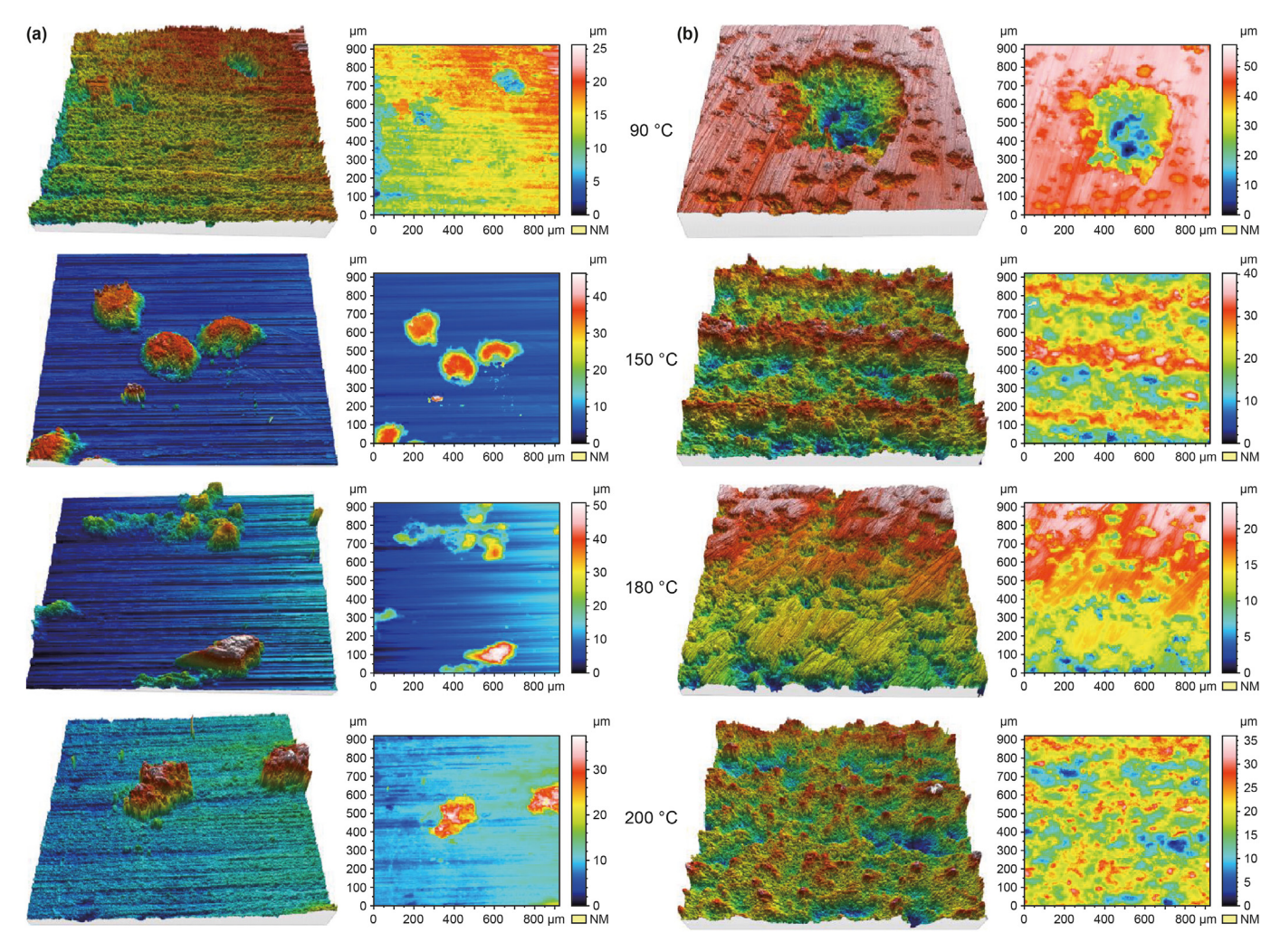


Fig. 12. (a) Casing sample morphology after damage by polysulfonated potassium drilling fluid; (b) Drilling tool sample morphology after damage by polysulfonated potassium drilling fluid.

drilling fluid on the damaged alloy samples. Due to the damage from the drilling fluid, the surface of the metal samples was covered with pits and abrasive wear marks, resulting in irregular rough surfaces. Therefore, polysulfonated potassium drilling fluid has better wettability on the surface of the samples (Xiao et al., 2022). As the temperature increases, the surface roughness shows an increasing trend, implying that the drilling fluid's adsorption on the sample's surface also increased.

From Fig. 21, it is evident that the contact angles of the drilling fluid on the samples, which were damaged by super-micro drilling fluid at different temperatures, display significant variations. Notably, the contact angle changes between the pre-damaged and post-damaged P110 steel samples are more pronounced when in contact with the drilling fluid. By comparing with the roughness data in Fig. 18, it can be deduced that samples with higher roughness levels exhibit better spreading of the super-micro drilling fluid on their surfaces. Additionally, the fine particles can also embed themselves on these rough surfaces.

#### 3.7. Wear and corrosion mechanism

Through a series of research methods, the damage to casing/ drilling tools during drilling fluid circulation is mainly categorized into irregular abrasion marks caused by sliding friction of solidphase particles in the drilling fluid on the metal surface, and pitting pits formed by ionic corrosion in the drilling fluid, with the former caused by friction between solid-phase particles and the metal surface while the latter by ionic corrosion in the drilling fluid. The mechanical damage process is illustrated in Figs. 22 and 23.

From Fig. 22, it is discernible that the metal samples exhibit irregular abrasion marks on their surface after being subjected to drilling fluid circulation. Under particulate wear conditions, as detailed in (Yang et al., 2018), mechanical calculation formulas suggest that when the particle size is smaller, it can more readily penetrate the metal surface, resulting in deeper abrasion marks. While solid phase components in different drilling fluid vary in particle size, microscopic morphologies indicate that the particles in super-micro drilling fluid are the smallest. Consequently, super-micro drilling fluid lead to the most significant abrasive wear on casings/drilling tools.

From Fig. 23, it becomes evident that the primary cause of corrosion is ionic corrosion. The drilling fluid contains an abundance of salts (such as KCl, used to inhibit the swelling of clay minerals). These salt molecules hydrolyze in the drilling fluid system into various ions, predominantly including Cl<sup>-</sup>, OH<sup>-</sup>. The primary corrosion products are FeCl<sup>-</sup> and Fe(OH)<sub>2</sub>. This corrosion

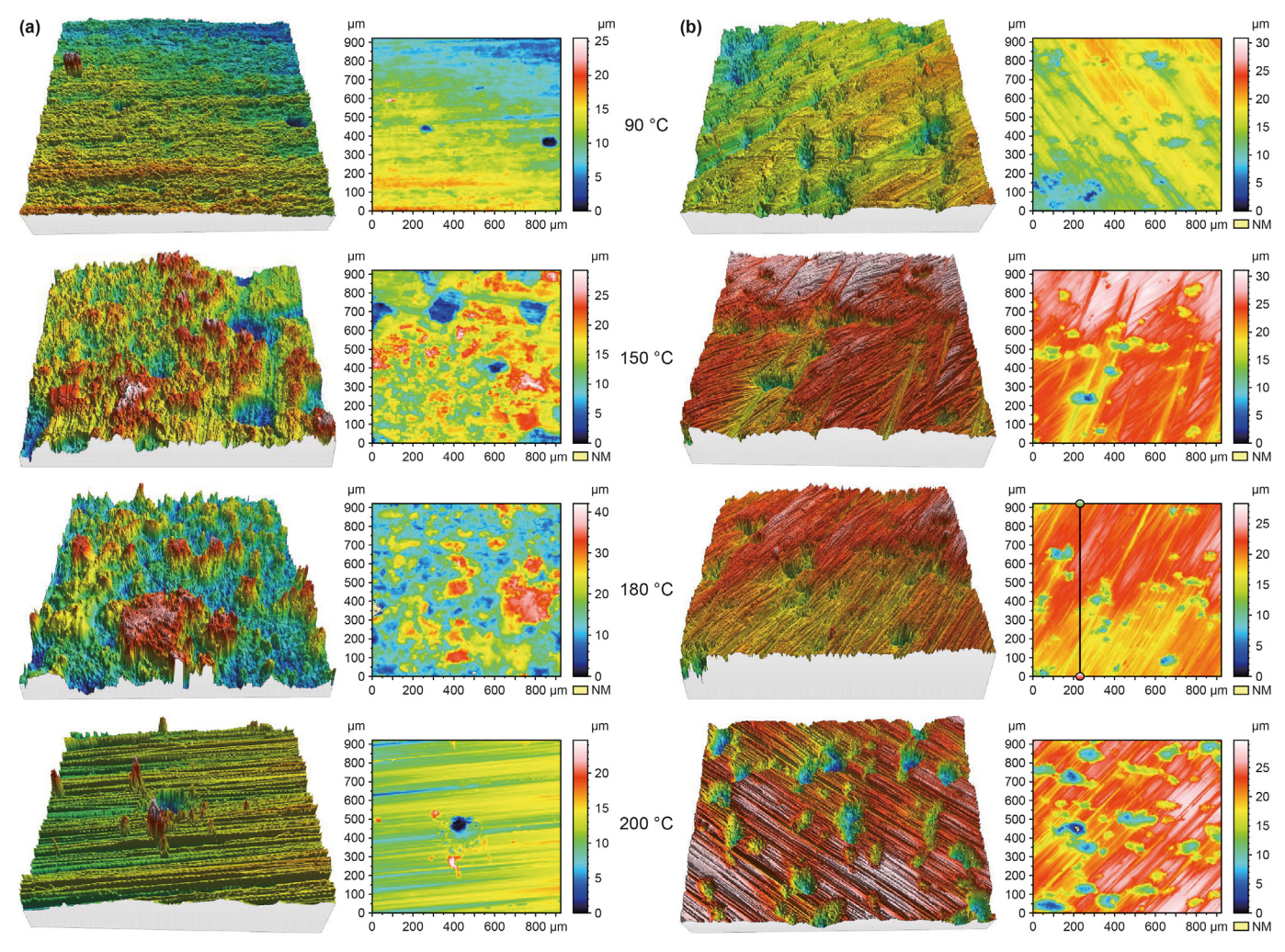


Fig. 13. (a) Casing sample morphology after super-micro drilling fluid damage; (b) Drilling tool sample morphology after super-micro drilling fluid damage.

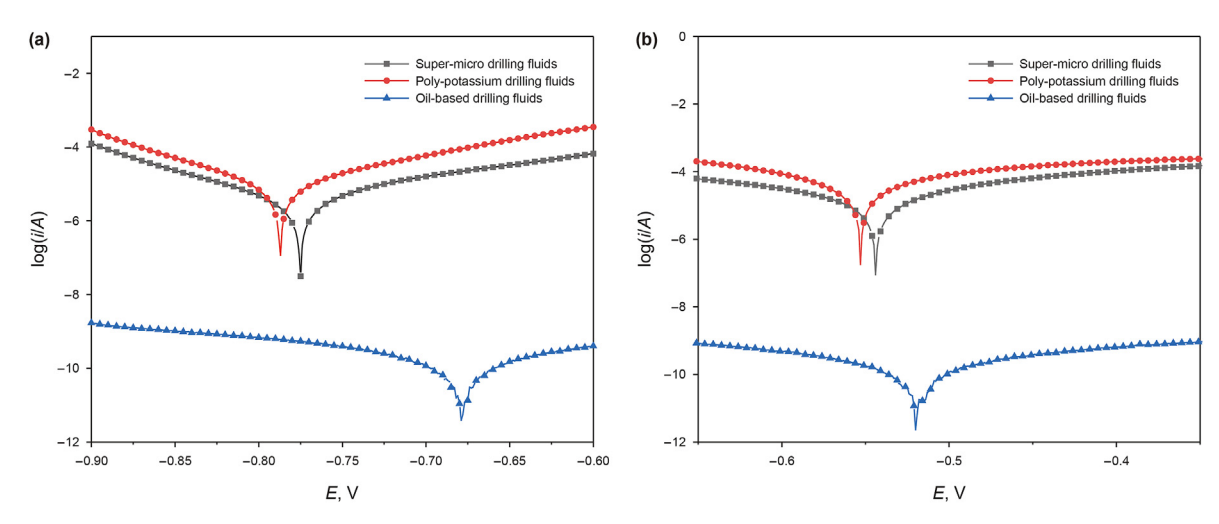
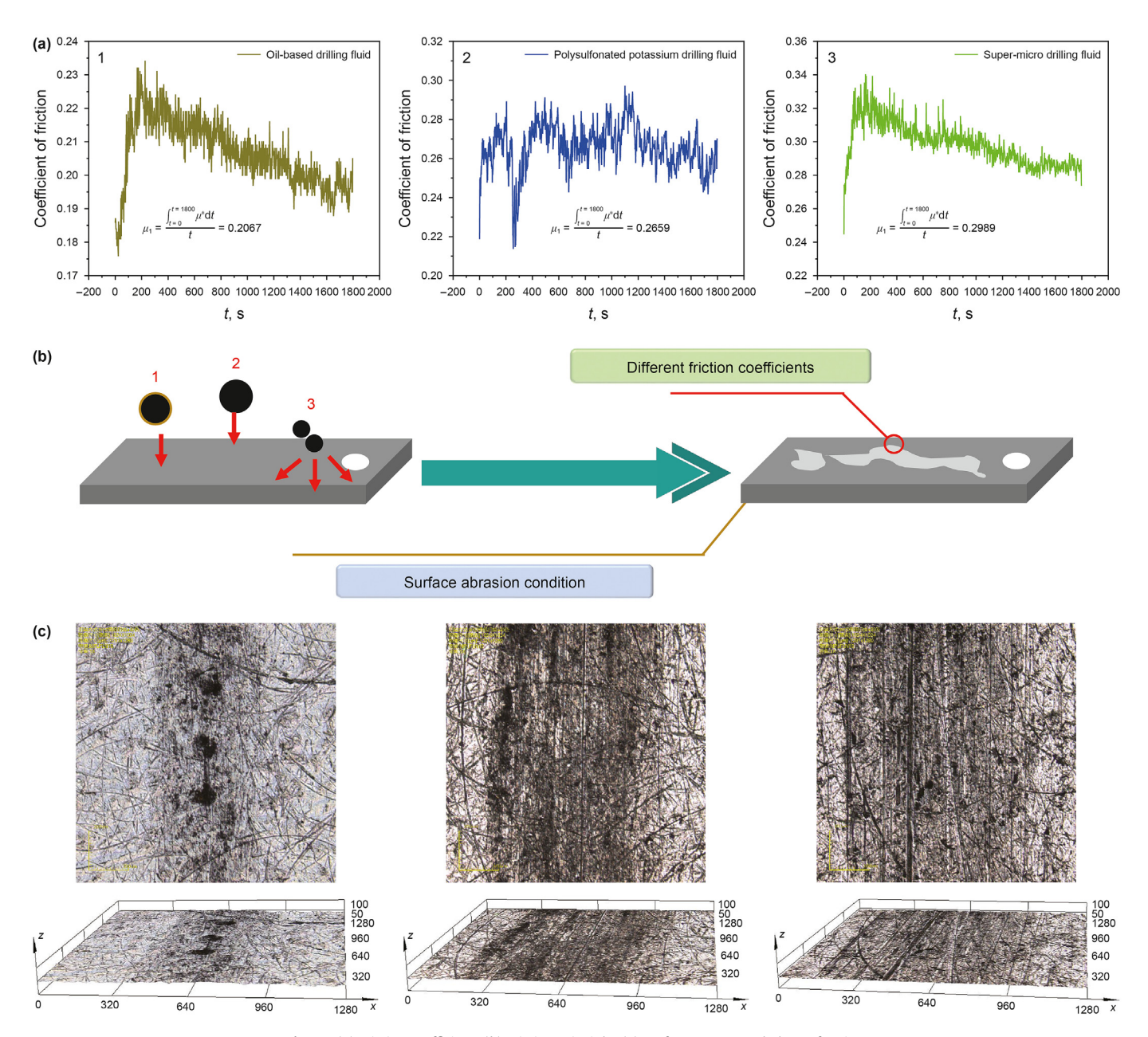
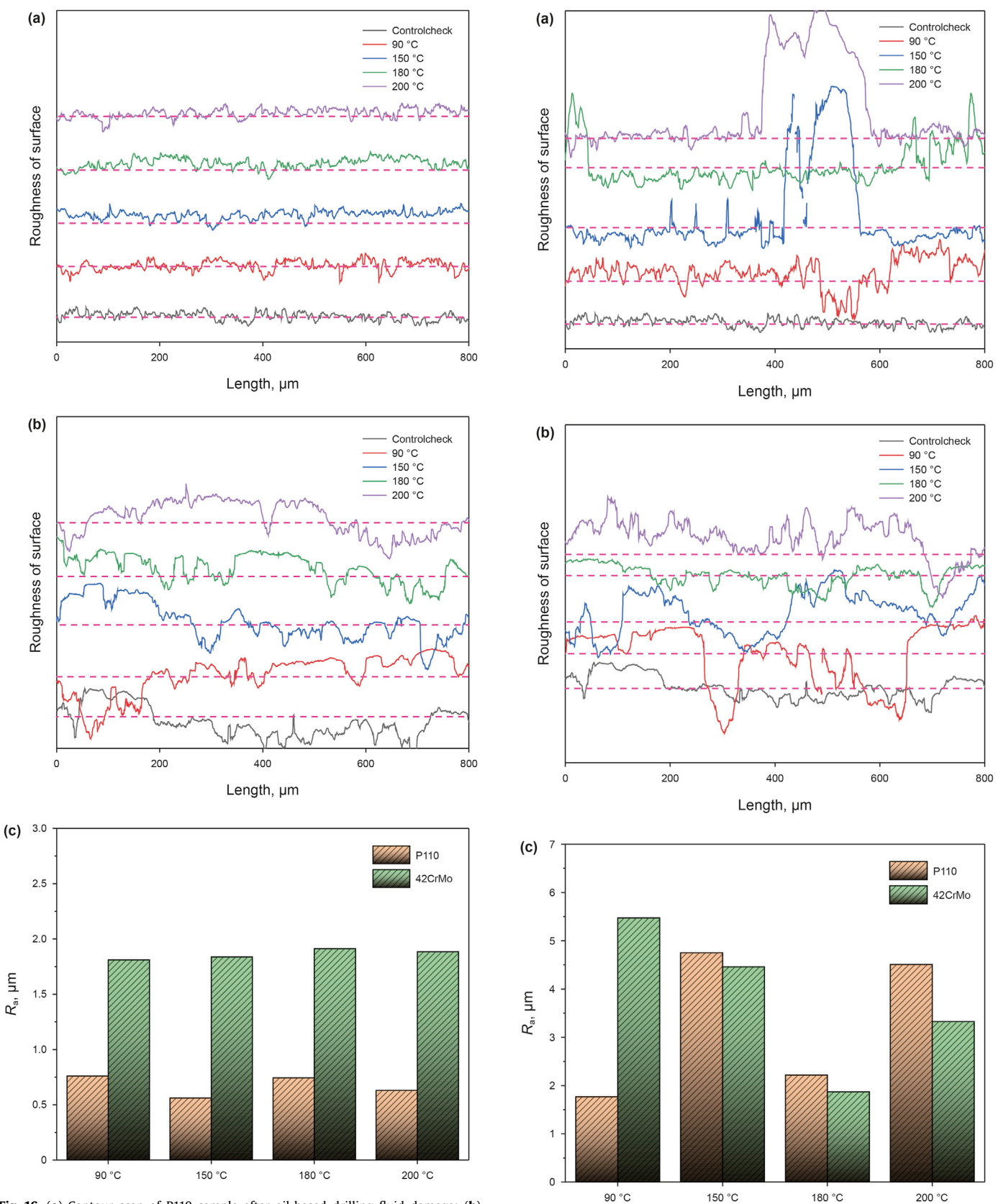


Fig. 14. (a) Polarization curves of metal samples for casing corroded by different types of drilling fluid; (b) Polarization curves of metal samples for drilling tools corroded by different types of drilling fluid.

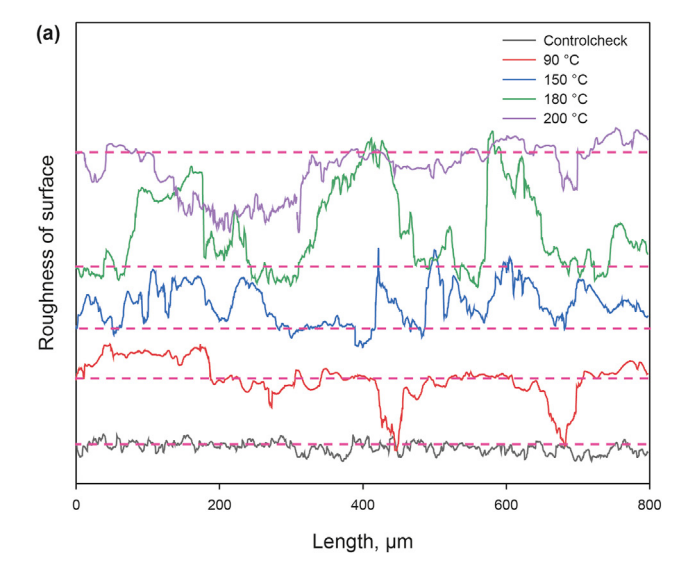


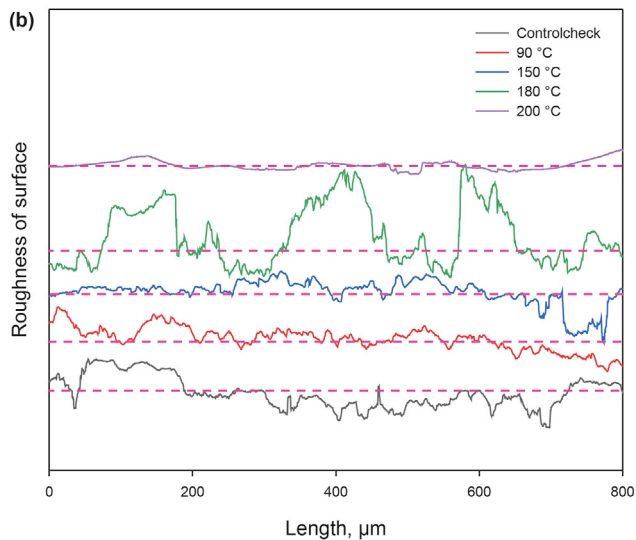
 $\textbf{Fig. 15. (a)} \ \ \textbf{Friction coefficient; (b)} \ \ \textbf{Friction principle; (c)} \ \ \textbf{Surface wear morphology of casing.}$ 



**Fig. 16.** (a) Contour scan of P110 sample after oil-based drilling fluid damage; (b) Contour scan of 42CrMo sample after oil-based drilling fluid damage; (c) Roughness of P110 sample and 42CrMo sample.

**Fig. 17.** (**a**) Contour scan of P110 sample after damage by polysulfone potassium drilling fluid; (**b**) Contour scan of 42CrMo sample after damage by polysulfone potassium drilling fluid; (**c**) Roughness of P110 sample and 42CrMo sample.





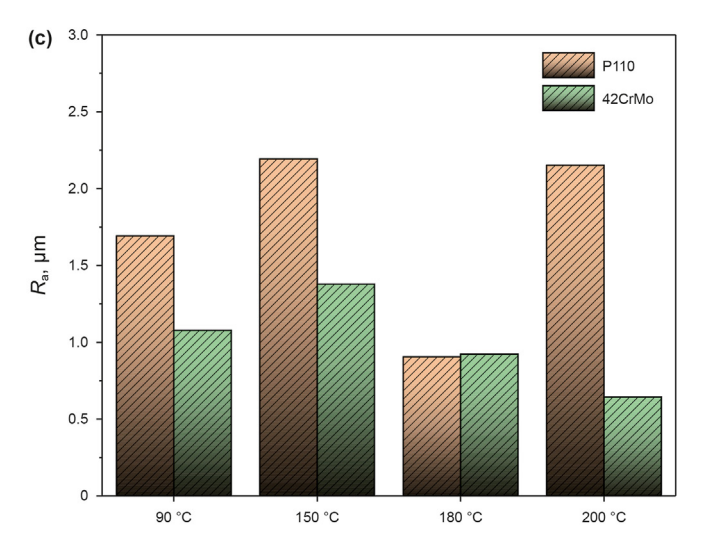


**Fig. 18.** (a) Contour scan of P110 sample after super-micro drilling fluid damage; (b) Contour scan of 42CrMo sample after super-micro drilling fluid damage; (c) Roughness of P110 sample and 42CrMo sample.

process forms numerous pitting sites on the metal surface, substantially compromising the metal's toughness and disrupting its surface structure (Sedmak et al., 2020).

Wear and corrosion occur concurrently and mutually reinforce each other. Pitting reduces the resilience of the metal surface, rendering it more susceptible to abrasion. Furthermore, wear disrupts the metal's protective oxide layer, accelerating the reaction between ions and the metal. This synergistic interplay between wear and corrosion results in heightened damage to the metal surface, which stands as a principal reason for the adverse effects of drilling fluid on casings/drilling tools.

This study conducts a systematic study on the wellbore pollution and damage caused by residual drilling fluid during ultra-deep well drilling. The pollution and damage mechanism of drilling fluid has profound guiding significance for wellbore cleaning work. We should choose environmentally friendly wellbore flushing fluid to clean the casing, thereby improving the service life of the casing and ensuring the cleanliness of the underground development environment.

#### 4. Conclusion

In this study, a systematic investigation was conducted on the contamination and damage to casings and drilling tools during the drilling process of ultra-deep wells using different types of drilling fluid (oil-based, polysulfonated potassium, and super-micro drilling fluid). Analysis of drilling fluid residues on the casings and drilling tools revealed that the primary constituents were solid-phase particles and organic components. As the bottom-hole temperature increased, the extent of damage to the casings and drilling tools decreased, with the least damage observed in the temperature range of 150–180 °C. Under varying temperatures, the surfaces of casings and tools damaged by different types of drilling fluid exhibited different roughness levels. Among them, the oil-based drilling fluid caused the least damage, primarily due to its high lubricity and the protective oil film it forms on metal surfaces, greatly mitigating harm to casings and tools. However, the oilbased fluid demonstrated strong adhesion, leading to more significant contamination. Polysulfonated potassium and super-micro drilling fluid, with their high solid-phase and ion content, inflicted considerable damage on casings and tools. The wettability of drilling fluid on the surfaces of casings and tools increased with surface roughness. Analyzing the mechanisms of damage by the drilling fluid, it was determined that the primary modes of damage to casings and tools stem from the abrasive wear caused by the solid-phase particles in the drilling fluid and corrosion due to its ions. The abrasive wear produces numerous scratches, while ionic corrosion results in extensive pitting. The combined effects of these mechanisms exacerbate the damage inflicted by the drilling fluid on casings and drilling tools.

#### **CRediT authorship contribution statement**

Han-Xuan Song: Writing — review & editing, Writing — original draft, Funding acquisition, Formal analysis, Data curation, Conceptualization. Shi-Ling Zhang: Funding acquisition. Xiang-Wei Chen: Writing — review & editing. Kiyingi Wyclif: Writing — review & editing. Ji-Xiang Guo: Funding acquisition. Rui-Ying Xiong: Writing — review & editing. Li Wang: Writing — review & editing.

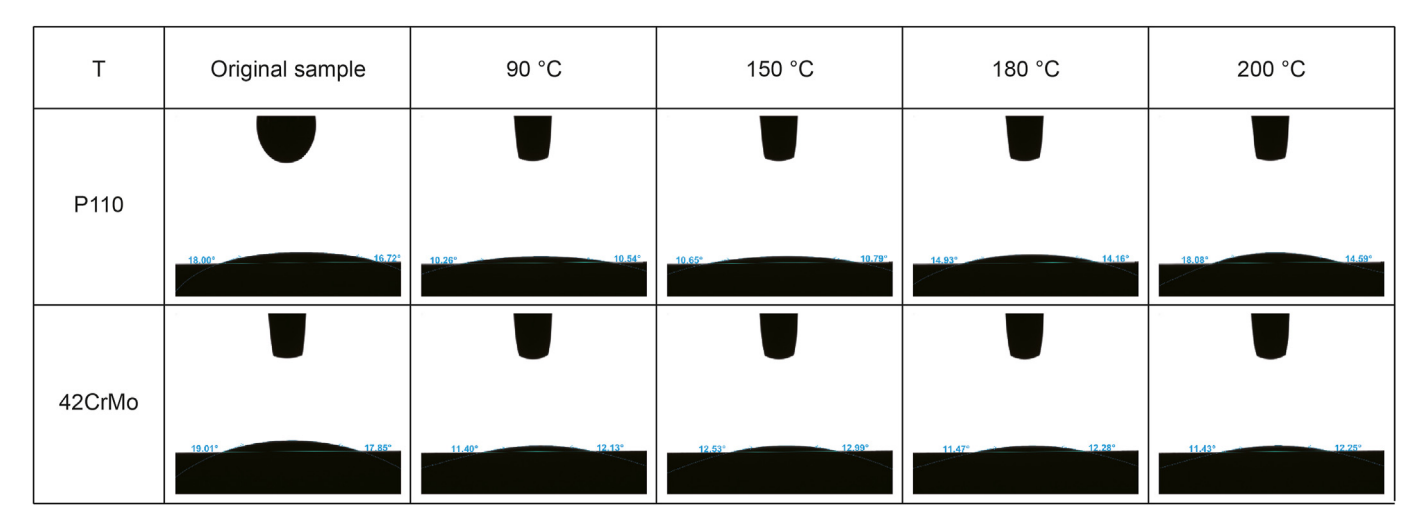


Fig. 19. Contact angle between the oil-based drilling fluid and post-damage metal samples.

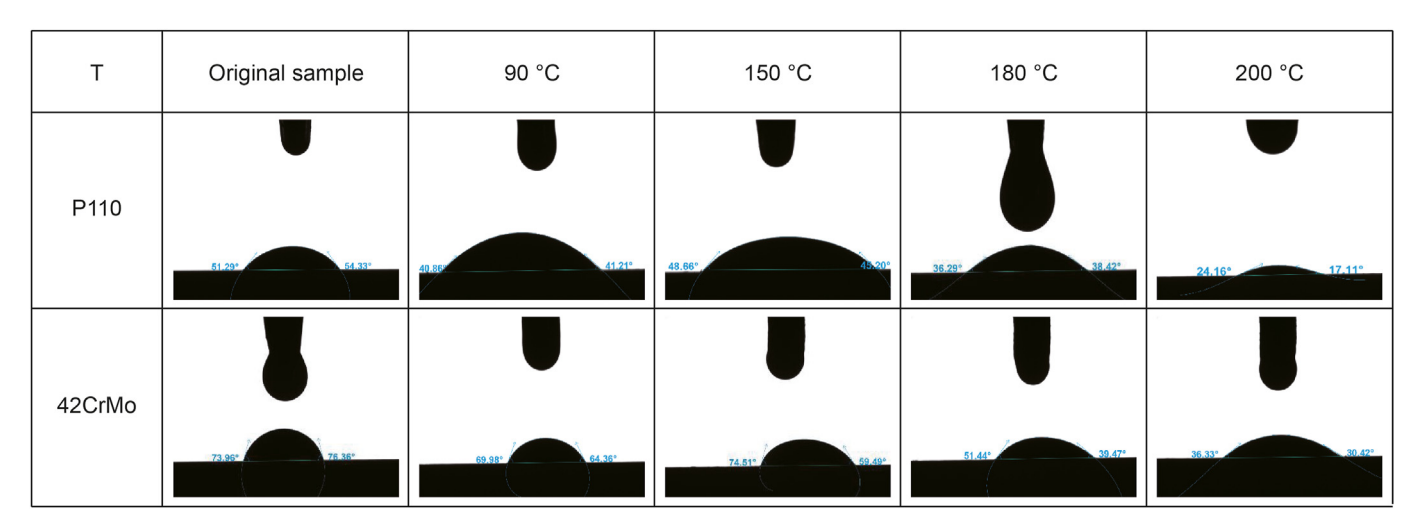


Fig. 20. Contact angle of polysulfonated potassium drilling fluid with post-damage metal samples.

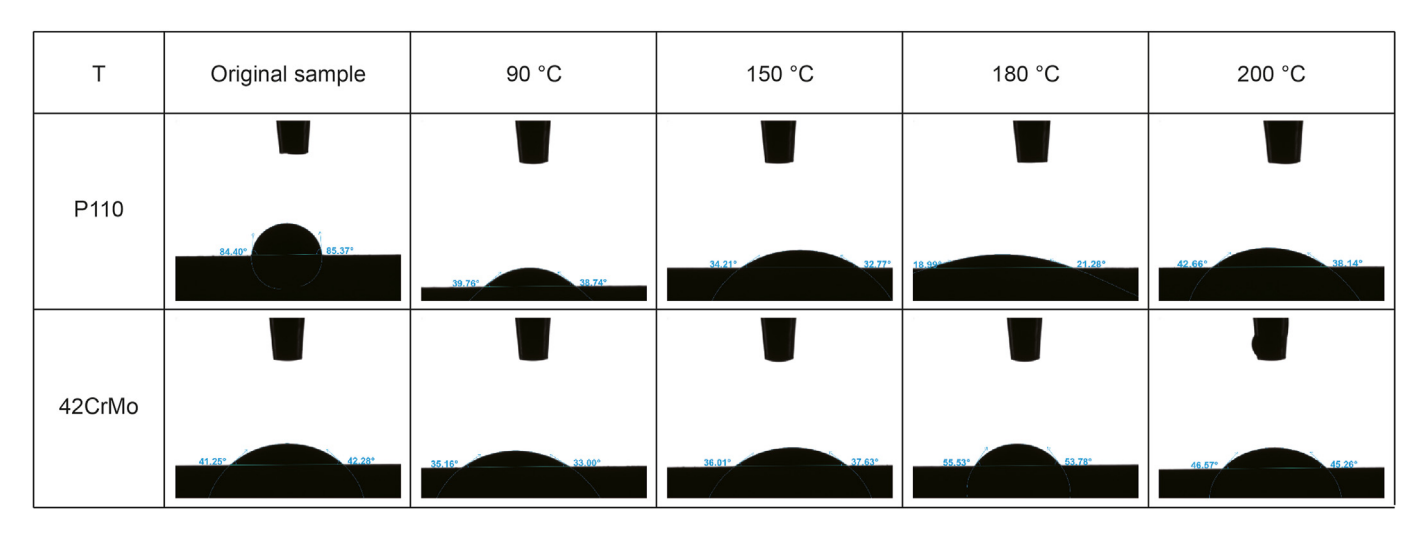


Fig. 21. Contact angle between the super-micro drilling fluid and post-damage metal samples.

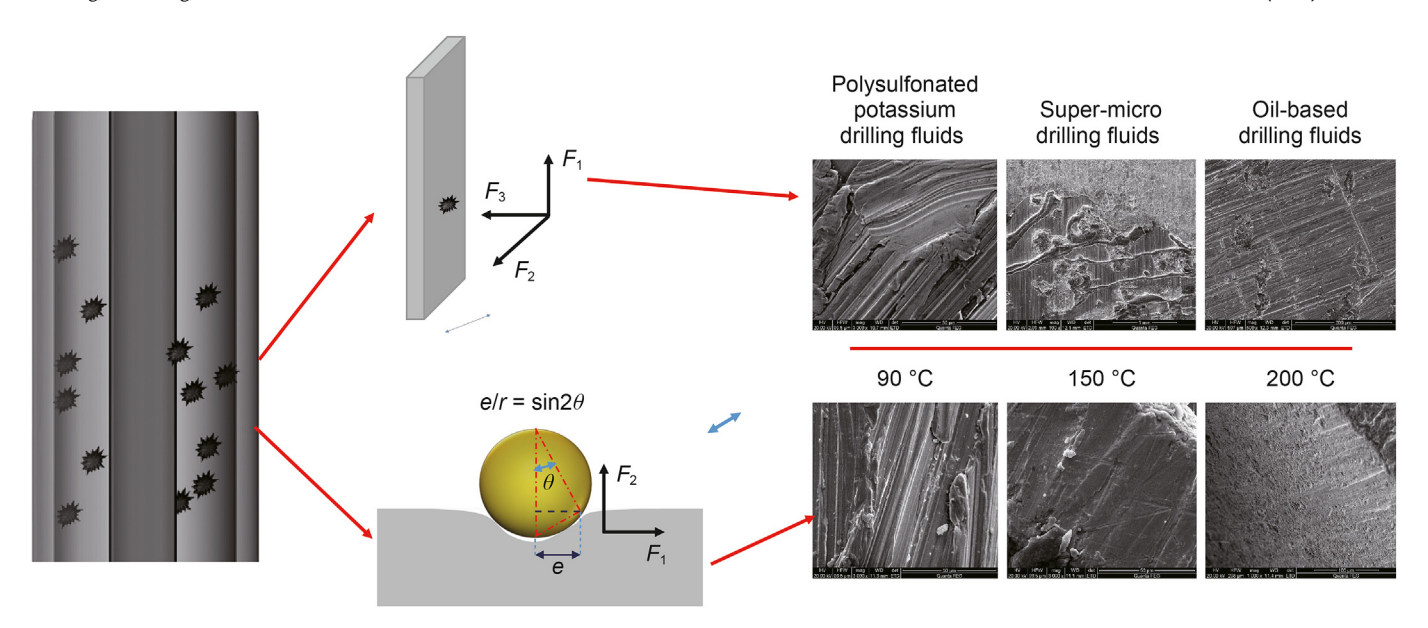
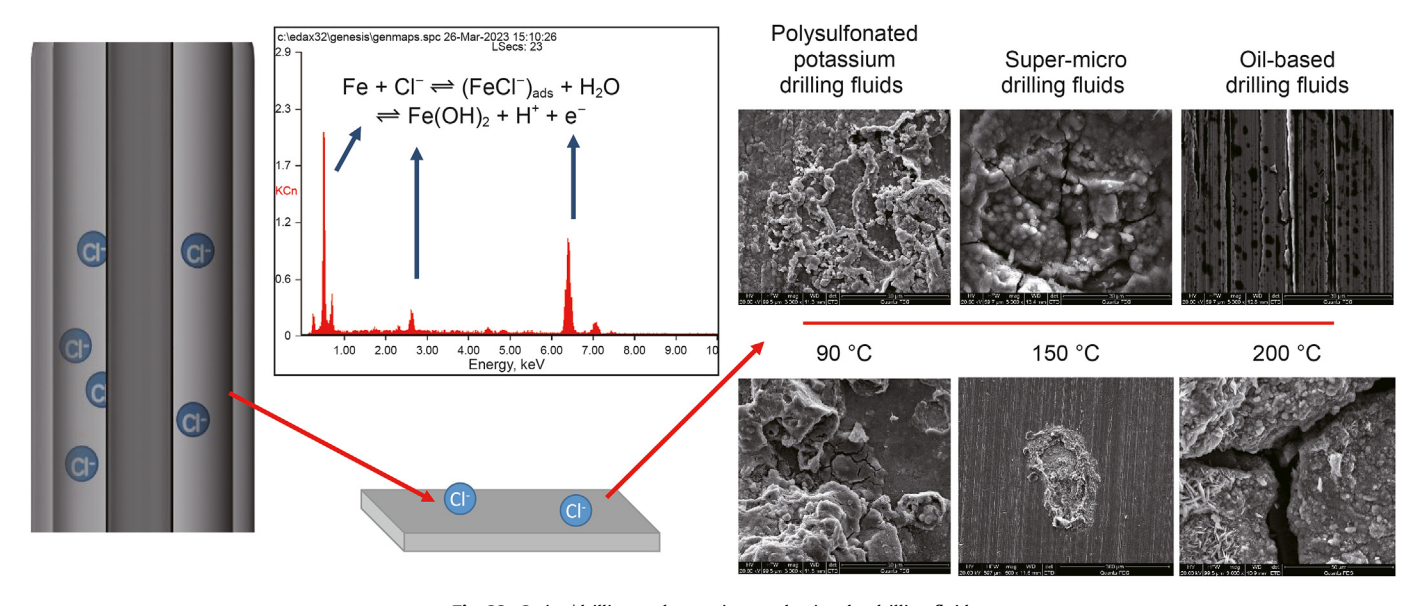


Fig. 22. Casing/drilling tool wear mechanism by solid phase abrasive particles in drilling fluid.



 $\textbf{Fig. 23.} \ \ \text{Casing/drilling tool corrosion mechanism by drilling fluid.}$ 

#### **Declaration of competing interest**

The authors declare that they have no known competing financial interests or personal relationships that could have appeared to influence the work reported in this paper.

#### Acknowledgments

This study received support and funding from the CNPC Project (2021ZG10), National Natural Science Foundation of China (No. 52174047) and Sinopec Project (No. P23138).

#### Nomenclature

AV Apparent viscosity
ES The electrical stability

*G'/G*" Storage modulus/Loss modulus

PV Plastic viscosity P110 P110 steel

YP Dynamic shear force

42CrMo 42CrMo steel

#### References

Anwar, I., Chojnicki, K., Bettin, G., Taha, M.R., Stormont, J.C., 2019. Characterization of wellbore casing corrosion product as a permeable porous medium. J. Pet. Sci. Eng. 180, 982–993. https://doi.org/10.1016/j.petrol.2019.05.087.

Berg, E., Sedberg, S., Kaarigstad, H., Omland, T.H., Svanes, K., 2006. Displacement of drilling fluids and cased-hole cleaning: what is sufficient cleaning? IADC/SPE Drilling Conference. SPE-99104-MS https://doi.org/10.2118/99104-MS.

Drilling Conference. SPE-99104-MS https://doi.org/10.2118/99104-MS.
Brege, J., El Sherbeny, W., Quintero, L., Jones, T., 2012. Using microemulsion technology to remove oil-based mud in wellbore displacement and remediation applications. North Africa Technical Conference and Exhibition. SPE-150237-MS. https://doi.org/10.2118/150237-MS.

Davoodi, S., Al-Shargabi, M., Wood, D.A., Rukavishnikov, V.S., Minaev, K.M., 2023. Thermally stable and salt-resistant synthetic polymers as drilling fluid additives for deployment in harsh sub-surface conditions: a review. J. Mol. Liq. 371,

- 121117. https://doi.org/10.1016/j.molliq.2022.121117.
- Deng, C., Du, G., Li, X., Xi, J., Lin, C., 2022. Effect of high temperature and high pressure on the biodegradability and biotoxicity of typical additives in drilling fluid. J. Pet. Sci. Eng. 208, 109773. https://doi.org/10.1016/j.petrol.2021.109773.
- Etrati, A., Roustaei, A., Frigaard, I.A., 2020. Strategies for mud-removal from washouts during cementing of vertical surface casing. J. Pet. Sci. Eng. 195, 107454. https://doi.org/10.1016/j.petrol.2020.107454.
- Feng, P., Borghesani, P., Smith, W.A., Peng, Z., 2020. Model-based surface roughness estimation using acoustic emission signals. Tribol. Int. 144, 106101. https:// doi.org/10.1016/j.triboint.2019.106101.
- Gautam, S., Guria, C., Rajak, V.K., 2022. A state of the art review on the performance of high-pressure and high-temperature drilling fluids: towards understanding the structure-property relationship of drilling fluid additives. J. Pet. Sci. Eng. 213, 110318. https://doi.org/10.1016/j.petrol.2022.110318.Guo, X., Hu, D., Li, Y., Duan, J., Zhang, X., Fan, X., Duan, H., Li, W., 2019. Theoretical
- Guo, X., Hu, D., Li, Y., Duan, J., Zhang, X., Fan, X., Duan, H., Li, W., 2019. Theoretical progress and key technologies of onshore ultra-deep oil/gas exploration. Engineering 5 (3), 458–470. https://doi.org/10.1016/j.eng.2019.01.012.
- Guo, X., Liu, J., Dai, L., Liu, Q., Fang, D., Wei, A., Wang, J., 2021. Friction-wear failure mechanism of tubing strings used in high-pressure, high-temperature and high-yield gas wells. Wear 468–469, 203576. https://doi.org/10.1016/j.wear.2020.203576.
- Humood, M., Ghamary, M.H., Lan, P., Iaccino, L.L., Bao, X., Polycarpou, A.A., 2019. Influence of additives on the friction and wear reduction of oil-based drilling fluid. Wear 422–423, 151–160. https://doi.org/10.1016/j.wear.2019.01.028.
- Ji, N., Zhao, M., Wu, Z., Wang, P., Feng, C., Xie, J., Long, Y., Song, W., Xiong, M., 2023. Collapse failure analysis of S13Cr-110 tubing in a high-pressure and high-temperature gas well. Eng. Fail. Anal. 148, 107187. https://doi.org/10.1016/jengfailanal.2023.107187
- Jia, H., Niu, C.C., Hu, Y.X., 2020. The potential study of ultra-high density heteropolysate solid free brine as well completion fluid for deep reservoir development. J. Nat. Gas Sci. Eng. 84, 103638. https://doi.org/10.1016/j.jngse.2020.103638.
- Jiang, G., Dong, T., Cui, K., He, Y., Quan, X., Yang, L., Fu, Y., 2022. Research status and development directions of intelligent drilling fluid technologies. Petrol. Explor. Dev. 49 (3), 660–670. https://doi.org/10.1016/s1876-3804(22)60055-7.
- Jing, Y., Wang, S., Chen, Y., Bao, M., Liu, L., 2018. Effect of corrosion product films induced by tensile stress on P110 casing steels induced in CO<sub>2</sub> environment. Int. J. Electrochem. Sci. 13 (8), 7629–7642. https://doi.org/10.20964/2018.08.21.
- Lin, T., Zhang, Q., Lian, Z., Chang, X., Zhu, K., Liu, Y., 2016. Evaluation of casing integrity defects considering wear and corrosion – application to casing design. J. Nat. Gas Sci. Eng. 29, 440–452. https://doi.org/10.1016/j.jngse.2016.01.029.
- Liu, J., Zhang, T., Sun, Y., Lin, D., Feng, X., Wang, F., 2022. Insights into the high temperature-induced failure mechanism of bentonite in drilling fluid. Chem. Eng. J. 445, 136680. https://doi.org/10.1016/j.cej.2022.136680.
- Luo, Y., Zhu, X., Liu, Y., Wang, X., Zhang, H., Li, B., Peng, Y., 2023. Effect of oil-based drilling fluid on the evolution of friction interface: a reactive molecular dynamics study at different temperatures. Tribol. Int. 188, 108820. https://doi.org/ 10.1016/j.triboint.2023.108820.
- Ma, Y., Cai, X., Yun, L., Li, Z., Li, H., Deng, S., Zhao, P., 2022. Practice and theoretical and technical progress in exploration and development of Shunbei ultra-deep

- carbonate oil and gas field, Tarim Basin, NW China. Petrol. Explor. Dev. 49 (1), 1–20. https://doi.org/10.1016/s1876-3804(22)60001-6.
- Mao, L., Cai, M., Liu, Q., Wang, G., 2020. Influence of oil-water ratio on the wear of Cr13 casing lubricated with drilling fluid. Mater. Today Commun. 25. https:// doi.org/10.1016/j.mtcomm.2020.101341.
- Mikhienkova, E.I., Lysakov, S.V., Neverov, A.L., Zhigarev, V.A., Minakov, A.V., Rudyak, V.Y., 2022. Experimental study on the influence of nanoparticles on oilbased drilling fluid properties. J. Pet. Sci. Eng. 208, 109452. https://doi.org/ 10.1016/j.petrol.2021.109452.
- Palimi, M.j., Tang, Y., Wu, M., Alvarez, V., Ghavidel, M., Kuru, E., Li, Q.Y., Li, W., Li, D.Y., 2022. Improve the tribo-corrosion behavior of oil-in-water emulsion-based drilling fluids by new derivatives of fatty acid-based green inhibitors. Tribol. Int. 174, 107723. https://doi.org/10.1016/j.triboint.2022.107723.
- Pu, L., Xu, P., Xu, M., Song, J., He, M., 2022. Lost circulation materials for deep and ultra-deep wells: a review. J. Pet. Sci. Eng. 214, 110404. https://doi.org/10.1016/ j.petrol.2022.110404.
- Quintero, L., Jones, T.A., Pietrangeli, G., 2011. Phase boundaries of microemulsion systems help to increase productivity. SPE European Formation Damage Conference. https://doi.org/10.2118/144209-MS. SPE-144209-MS.
- Sedmak, A., Arsić, M., Šarkoćević, Ž., Medjo, B., Rakin, M., Arsić, D., Lazić, V., 2020.
  Remaining strength of API J55 steel casing pipes damaged by corrosion. Int. J.
  Pres. Ves. Pip. 188, 104230. https://doi.org/10.1016/j.ijpvp.2020.104230.
- Sun, J., Zhang, X., Lv, K., Liu, J., Xiu, Z., Wang, Z., Huang, X., Bai, Y., Wang, J., Jin, J., 2022. Synthesis of hydrophobic associative polymers to improve the rheological and filtration performance of drilling fluids under high temperature and high salinity conditions. J. Pet. Sci. Eng. 209, 109808. https://doi.org/10.1016/j.petrol.2021.109808.
- Wan, H., Li, S., Li, J., Liu, T., Lin, J., Min, J., 2023. Wettability transition of metallic surfaces from laser-generated superhydrophilicity to water-induced superhydrophobicity via a facile and eco-friendly strategy. Mater. Des. 226, 111691. https://doi.org/10.1016/j.matdes.2023.111691.
- Wang, C., Meng, R., Xiao, F., Wang, R., 2016. Use of nanoemulsion for effective removal of both oil-based drilling fluid and filter cake. J. Nat. Gas Sci. Eng. 36, 328–338. https://doi.org/10.1016/j.jngse.2016.10.035.
- Xiao, Y., Zheng, J., He, Y., Wang, L., 2022. Droplet and bubble wetting behaviors: the roles of surface wettability and roughness. Colloids Surf., A 653, 130008. https:// doi.org/10.1016/j.colsurfa.2022.130008.
- Yanagisawa, N., Masuda, Y., Asanuma, H., Osato, K., Sakura, K., 2021. Estimation of casing material corrosion rates for supercritical geothermal development. Geothermics 96, 102149. https://doi.org/10.1016/j.geothermics.2021.102149.
- Yang, L., Wang, D., Guo, Y., 2018. Frictional behaviors of iron based tools-casing with sand deposition. Tribol. Int. 123, 180–190. https://doi.org/10.1016/j.triboint.2018.03.013.
- Zhang, Z., Scherer, G.W., Prod'Homme, R.K., Choi, M., 2018. Effect of casing surface roughness on the removal efficiency of non-aqueous drilling fluids. J. Nat. Gas Sci. Eng. 51, 155–165. https://doi.org/10.1016/j.jngse.2018.01.004.
- Zhang, Z., Wei, Y., Xiong, Y., Peng, G., Wang, G., Lu, J., Zhong, L., Wang, J., 2022. Influence of the location of drilling fluid loss on wellbore temperature distribution during drilling. Energy 244, 123031. https://doi.org/10.1016/j.energy.2021.123031.